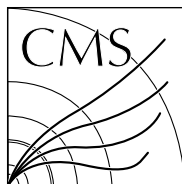


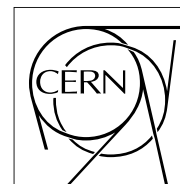
Available on CMS information server

**CMS DP -2016/063**

The Compact Muon Solenoid Experiment

# CMS Performance Note

Mailing address: CMS CERN, CH-1211 GENEVA 23, Switzerland

**29 September 2016 (v2, 03 October 2016)**

## CMS Tracker Alignment Performance Results Summer 2016

CMS Collaboration

### Abstract

The tracking system of the CMS detector provides excellent resolution for charged particle tracks and an efficient way of tagging jets. In order to reconstruct good quality tracks, the position and orientation of each silicon pixel and strip modules need to be determined with a precision of several micrometers. The performance of the CMS tracker alignment in 2016 using cosmic-ray data recorded at 0 T magnetic field and proton-proton collision data recorded at 3.8 T magnetic field has been studied. The data-driven validation of the results are presented. The time-dependent movement of the pixel detector's large-scale structure is demonstrated.

# CMS Tracker Alignment Performance Results Summer 2016

---

The CMS Collaboration

cms-dpg-conveners-tracker@cern.ch

twiki : <https://twiki.cern.ch/twiki/bin/view/CMSPublic/TkAlignmentPerformanceICHEP2016>

July 2016

# Introduction

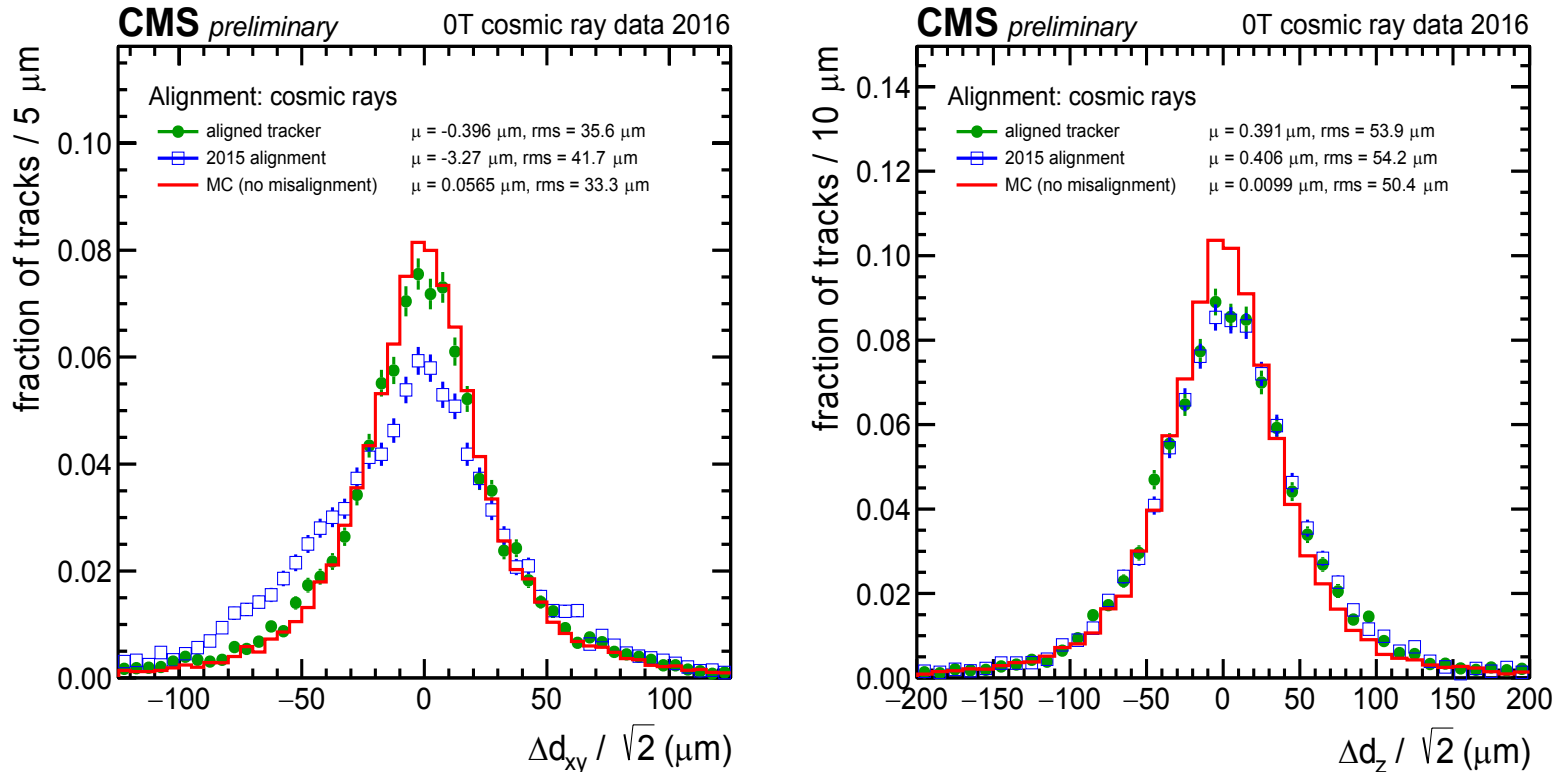
- Two new aligned objects presented:
  - Cosmics data at 0T
  - Cosmics + collision data at 3.8T
  - They correspond to different detector geometries particularly due to changes of the magnetic field.
- Alignments under study are the result of a global (Millepede-II) [1,2] and local (HipPy) fit approach [2]
  - The results are obtained by different approaches of running the two algorithms in sequence. In each data-taking period, the starting point for the alignment fit is the alignment obtained in the previous data-taking period.
  - In addition, the two algorithms run independently confirm each other.

# Cosmic-Track Splitting Validation

Cosmic ray tracks are split in half at the hit closest to origin and refitted with the alignment constants under consideration. The differences in various track parameters between the two half-tracks are studied.

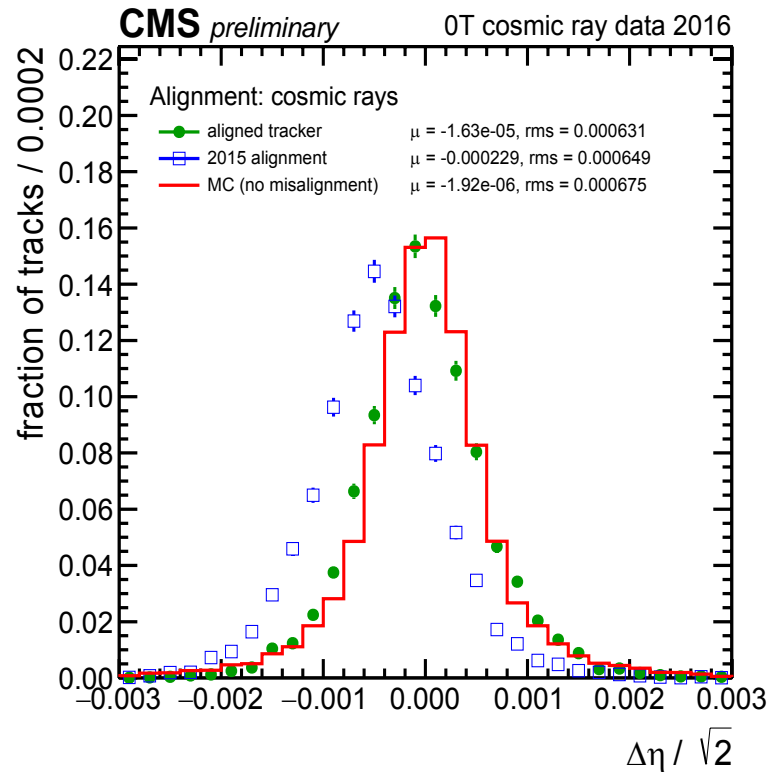
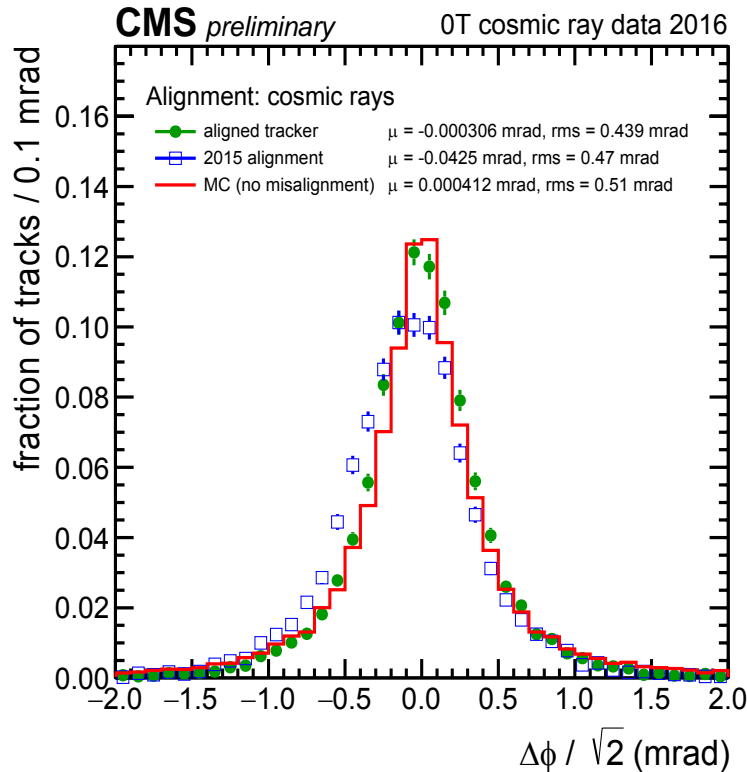
The width of the distribution measures the achieved alignment precision, while deviations from zero indicate possible biases.

# 0T Cosmic-Ray Data : Track Splitting



The normalized differences between two halves of a cosmic track, split at the point of closest approach to the interaction region, in  $d_{xy}$ , the xy distance, and  $d_z$ , the z distance, between the track and the origin. The observed precision using the aligned geometry (green circles), produced with the Millepede-II and HipPy algorithms using cosmic ray data at 0T, is a major improvement over the 2015 EOY geometry (blue empty squares) which is no longer valid for 2016 data, primarily because of temperature and magnetic field changes. The mean and rms values, calculated in the plotting range, show that the bias is reduced compared with 2015 geometry, and the precision comes close to that of the ideal Monte Carlo, illustrating that the tracker has almost reached its design spatial and angular resolution for 0T cosmic ray data.

# 0T Cosmic-Ray Data : Track Splitting



The normalized differences between two halves of a cosmic track, split at the point of closest approach to the interaction region, in the track's azimuthal angle  $\varphi$  and polar angle  $\eta$ . The observed precision using the aligned geometry (green circles), produced with the Millepede-II and HipPy algorithms using cosmic ray data at 0T, is a major improvement over the 2015 EOY geometry (blue empty squares) which is no longer valid for 2016 data, primarily because of temperature and magnetic field changes. The mean and rms values, calculated in the plotting range, show that the bias is reduced compared with 2015 geometry, and the precision comes close to that of the ideal Monte Carlo, illustrating that the tracker has almost reached its design spatial and angular resolution for 0T cosmic ray data.

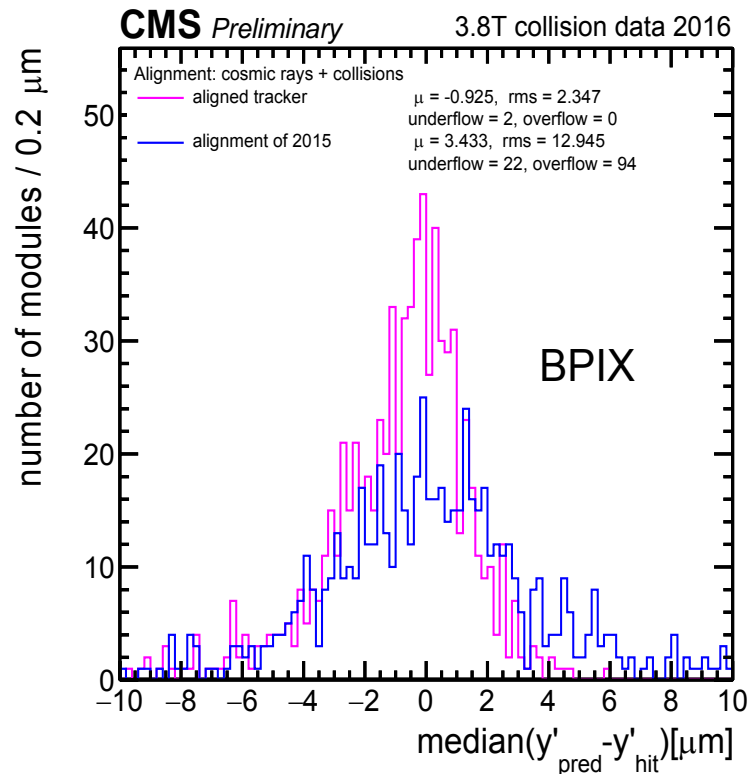
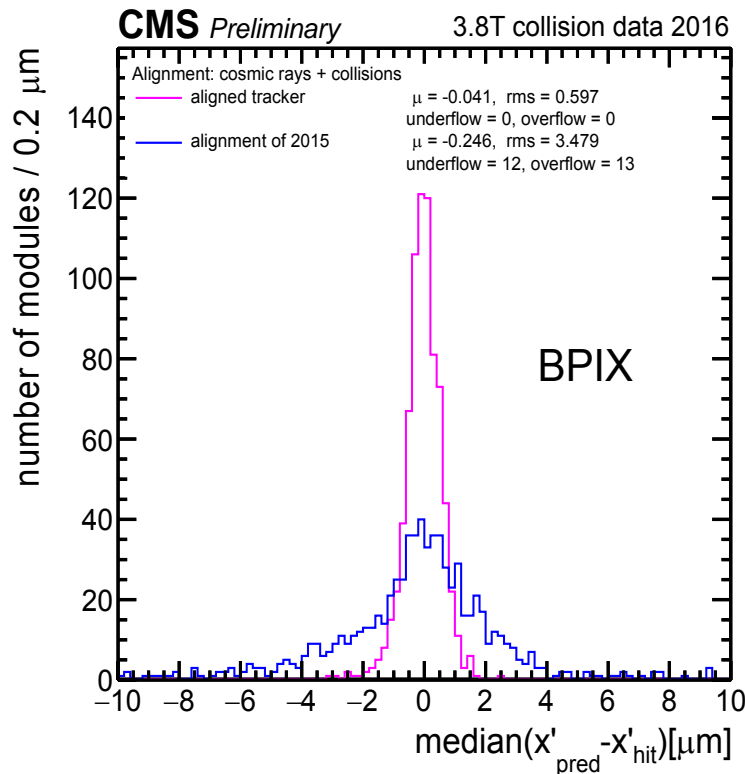
# DMR Validation

## - Distributions of medians of unbiased track-hit residuals

Each track is refitted using the alignment constants under consideration, and the hit prediction for each module is obtained from all of the other track hits. The median of the distribution of unbiased hit residuals is then taken for each module and is histogrammed.

The width of this distribution of the medians of residuals (DMR) is a measure of the statistical precision of alignment results; deviations from zero indicate possible biases. The width also has an intrinsic component due to the limited number of tracks, meaning that distributions can only be compared if they are produced with the same number of tracks, as is the case within each set of plots here.

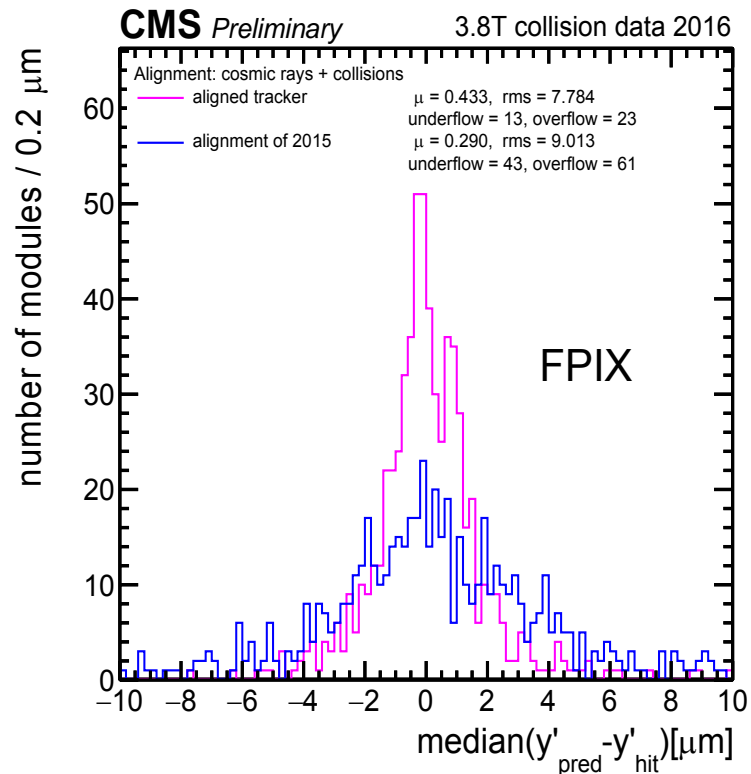
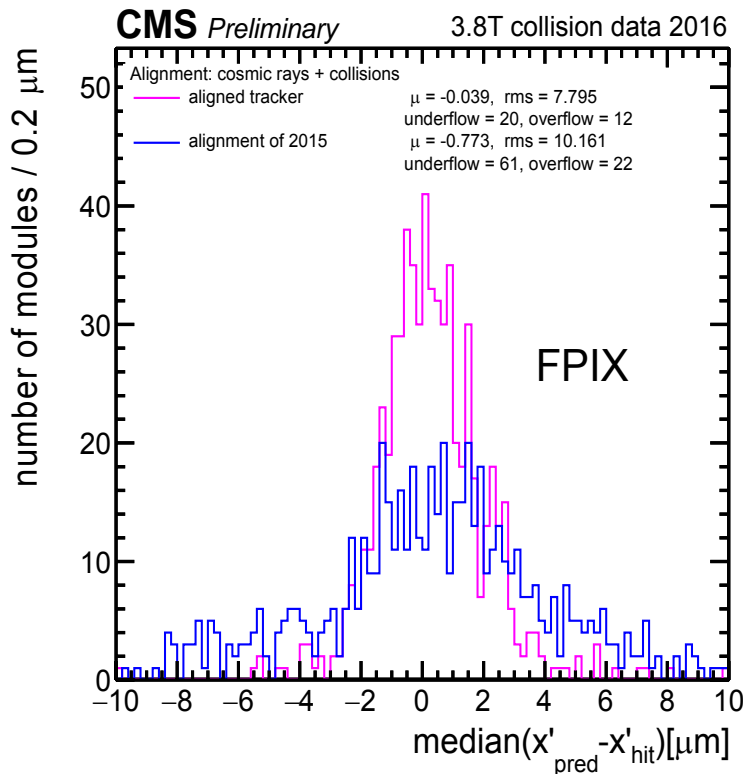
# 3.8T Collision Data DMR : BPIX



The distribution of median residuals is plotted for the local x- and y-directions in the barrel pixel detector, using 1 million collisionary events collected with the magnetic field at 3.8T. The blue line shows the geometry obtained at the end of 2015, which is no longer valid for 2016 data, primarily because of temperature and magnetic field changes. The alignment shown in magenta was produced with the Millepede-II and HipPy algorithms using 3.8T cosmic ray and collision data. The position of the pixel detector is known to be very sensitive to the change of conditions. The rms values, calculated using modules both inside and outside the plot range, show improvement over the 2015 geometry by a factor of 5.

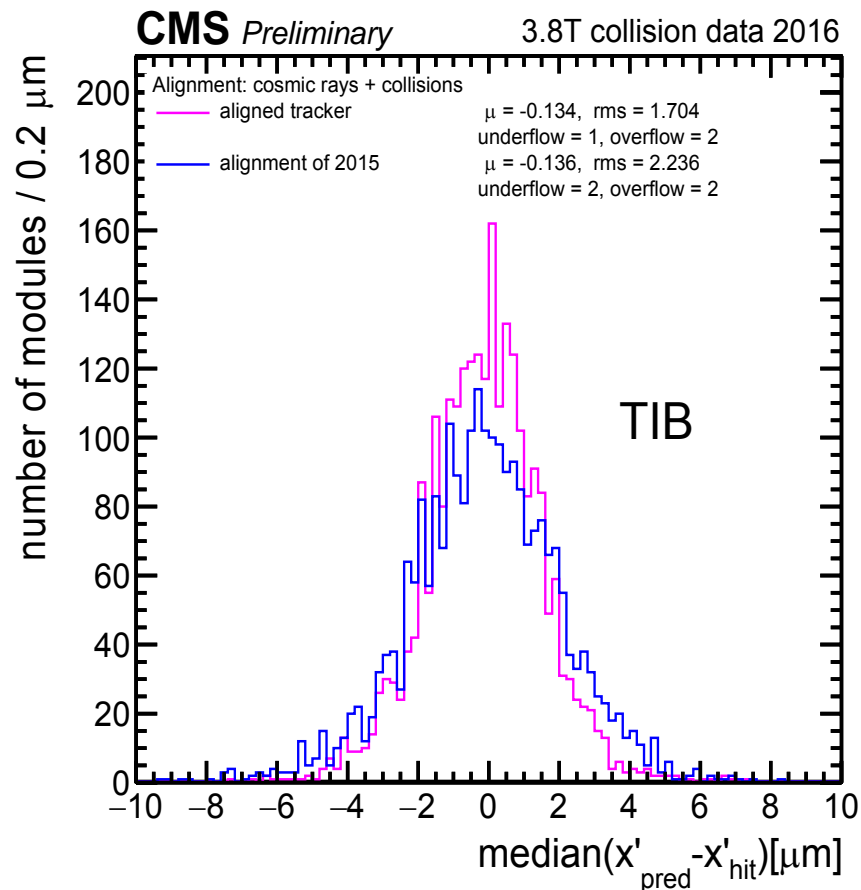


# 3.8T Collision Data DMR : FPIX



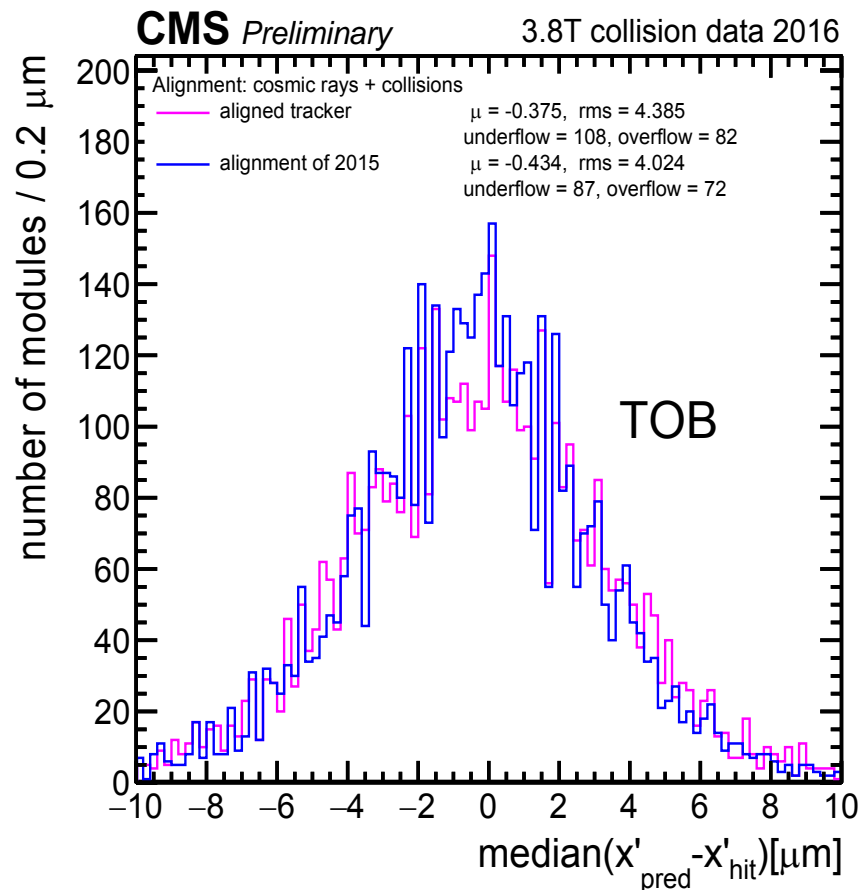
The distribution of median residuals is plotted for the local x- and y-directions in the forward pixel detector, using 1 million collision events collected with the magnetic field at 3.8T. The blue line shows the geometry obtained at the end of 2015, which is no longer valid for 2016 data, primarily because of temperature and magnetic field changes. The alignment shown in magenta was produced with the Millepede-II and HipPy algorithms using 3.8T cosmic ray and collision data. The position of the pixel detector is known to be very sensitive to the change of conditions. The rms values, calculated using modules both inside and outside the plot range, show improvement over the 2015 geometry.

## 3.8T Collision Data DMR : TIB



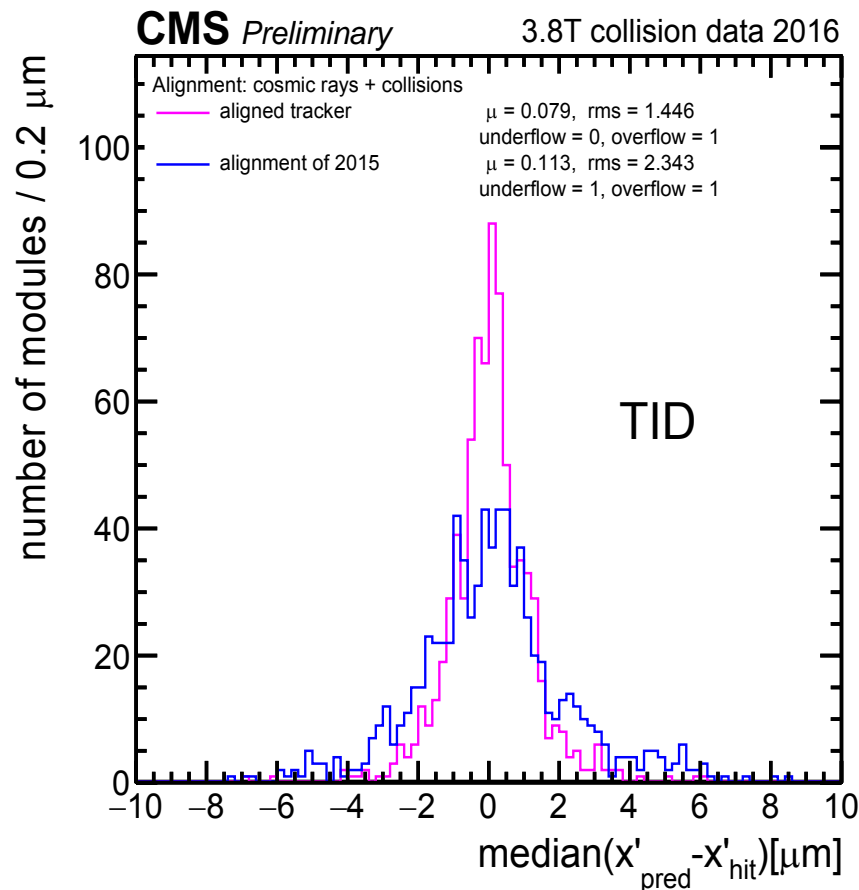
The distribution of median residuals is plotted for the tracker inner barrel, using 1 million collision events collected with the magnetic field at 3.8T. The blue line shows the geometry obtained at the end of 2015, which is no longer valid for 2016 data, primarily because of temperature and magnetic field changes. The alignment shown in magenta was produced with the Millepede-II and HipPy algorithms using 3.8T cosmic ray and collision data. The rms values, calculated using modules both inside and outside the plot range, show improvement over the 2015 geometry.

## 3.8T Collision Data DMR : TOB



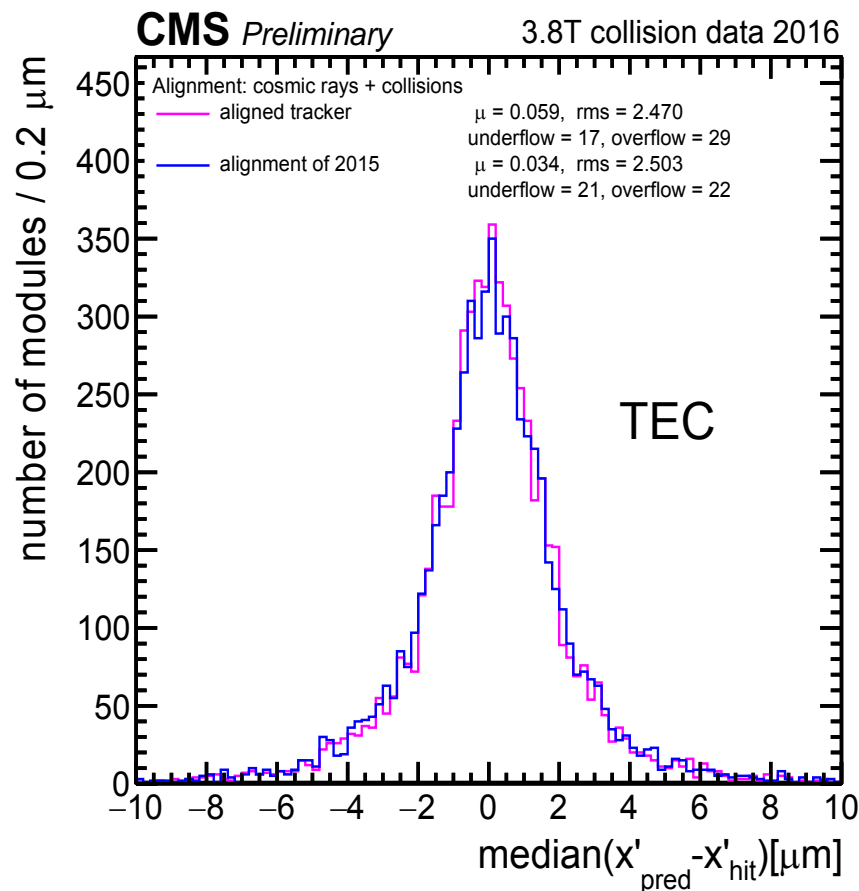
The distribution of median residuals is plotted for the tracker outer barrel, using 1 million collision events collected with the magnetic field at 3.8T. The blue line shows the geometry obtained at the end of 2015, which is no longer valid for 2016 data, primarily because of temperature and magnetic field changes. The alignment shown in magenta was produced with the Millepede-II and HipPy algorithms using 3.8T cosmic ray and collision data. The tracker outer barrel is the most stable part of the tracker, and it is used as a reference for the alignment algorithm. Therefore the rms values, calculated using modules both inside and outside the plot range, do not differ much for the two geometries.

## 3.8T Collision Data DMR : TID



The distribution of median residuals is plotted for the tracker inner disks, using 1 million collision events collected with the magnetic field at 3.8T. The blue line shows the geometry obtained at the end of 2015, which is no longer valid for 2016 data, primarily because of temperature and magnetic field changes. The alignment shown in magenta was produced with the Millepede-II and HipPy algorithms using 3.8T cosmic ray and collision data. The rms values, calculated using modules both inside and outside the plot range, show improvement over the 2015 geometry.

## 3.8T Collision Data DMR : TEC



The distribution of median residuals is plotted for the tracker endcaps, using 1 million collision events collected with the magnetic field at 3.8T. The blue line shows the geometry obtained at the end of 2015, which is no longer valid for 2016 data, primarily because of temperature and magnetic field changes. The alignment shown in magenta was produced with the Millepede-II and HipPy algorithms using 3.8T cosmic ray and collision data. The 2016 geometry does not contain an update of the position of the single modules in the tracker endcaps, therefore the rms values, calculated using modules both inside and outside the plot range, do not differ much for the two geometries.

# Primary Vertex Validation

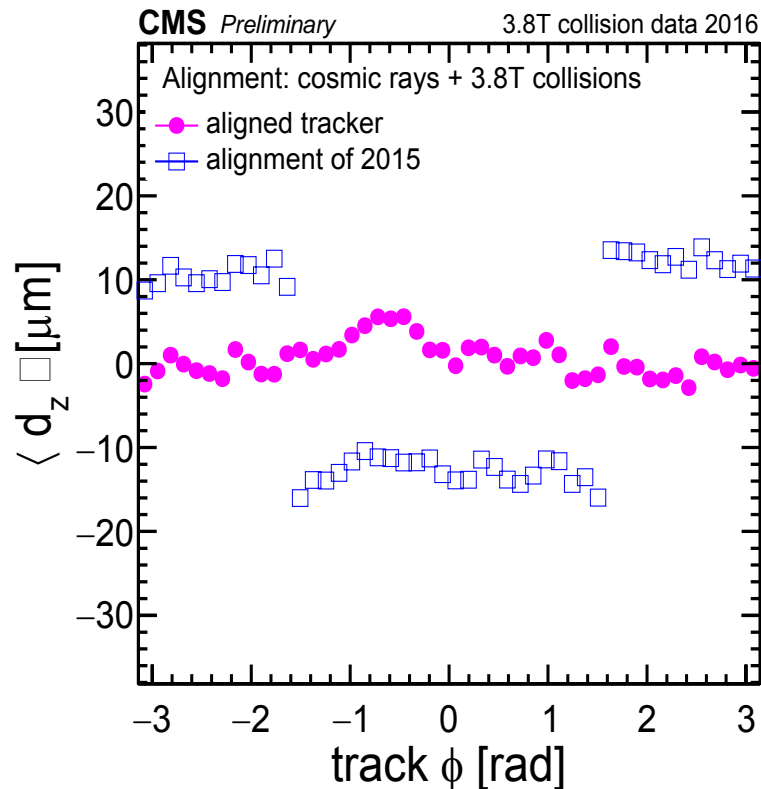
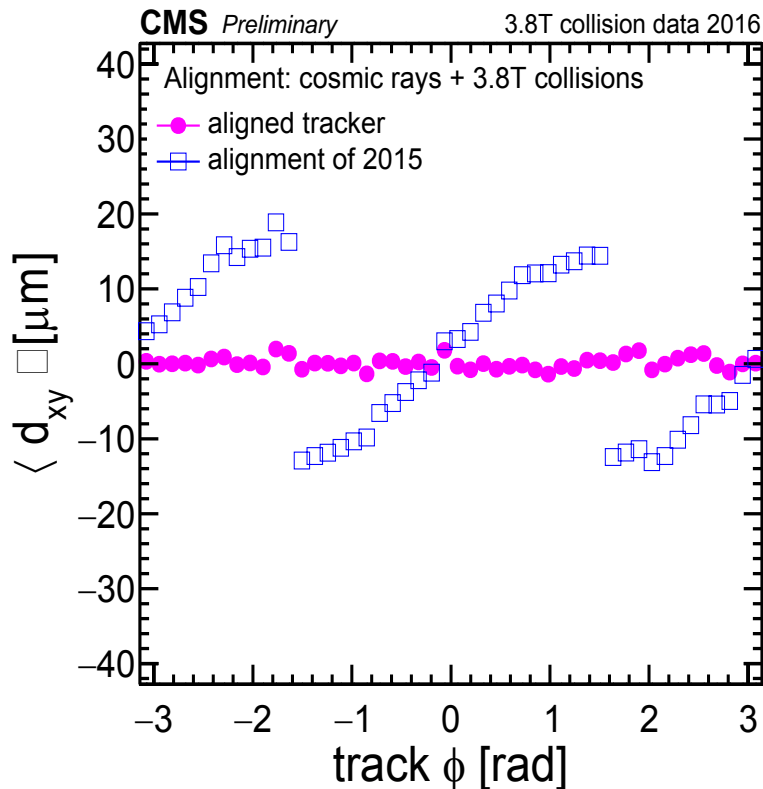
The resolution of the reconstructed vertex position is driven by the pixel detector since it is the closest detector to the interaction point and has the best hit resolution. The primary vertex residual method is based on the study the distance between the track and the vertex, the latter reconstructed without the track under scrutiny (unbiased track-vertex residual).

Selection and reconstruction of the events is the following:

- Events used in this analysis are selected online with minimum bias triggers.
- The fit of the vertex must have at least 4 degrees of freedom.
- For each of the vertices, the impact parameters are measured for tracks with:
  - more than 6 hits in the tracker, of which at least two are in the pixel detector,
  - at least one hit in the first layer of the Barrel Pixel or the first disk of the Forward Pixel,
  - $\text{Chi}^2/\text{ndof}$  of the track fit  $< 5$ .
- The vertex position is recalculated excluding the track under scrutiny.
- A deterministic annealing clustering algorithm is used in order to make the method robust against pileup, as in the default reconstruction sequence.

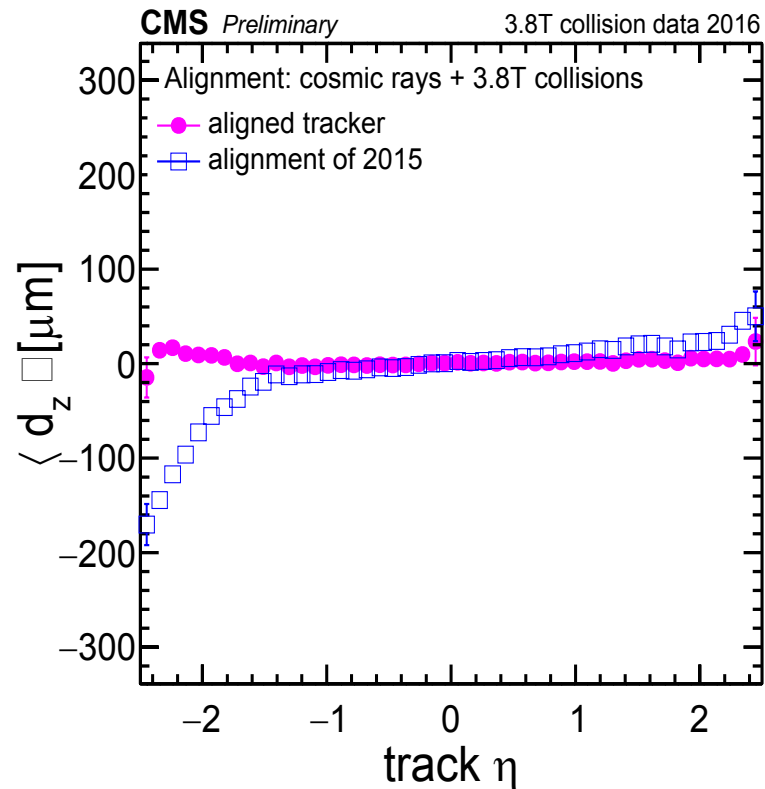
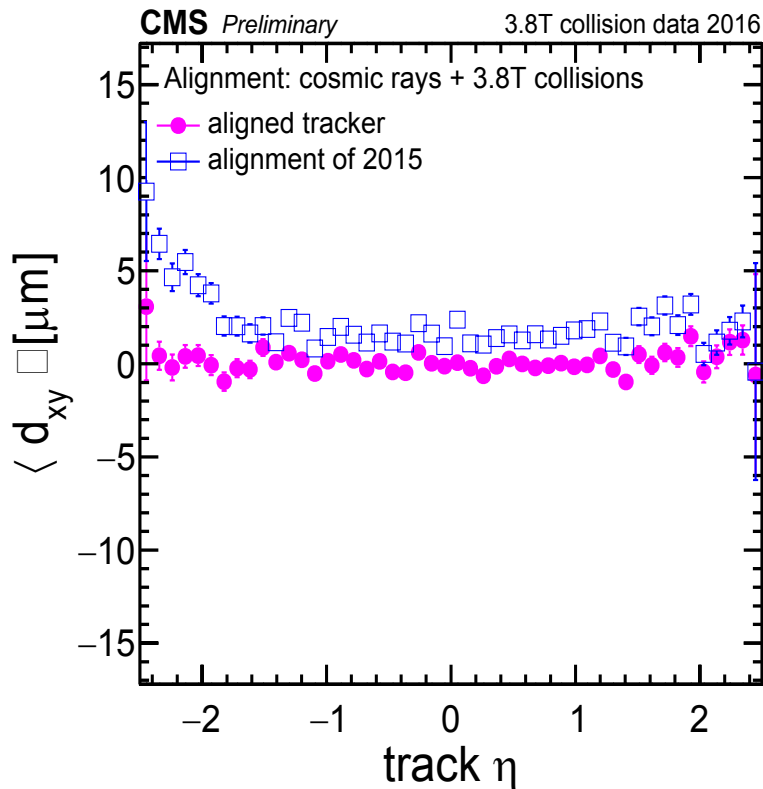
The distributions of the unbiased track-vertex residuals in the transverse plane, and in the longitudinal direction, are studied in bins of track azimuth  $\varphi$  and pseudo-rapidity  $\eta$ . Random misalignments of the modules affect only the resolution of the unbiased track-vertex residual, increasing the width of the distributions, but without biasing their mean. Systematic movements of the modules will bias the distributions in a way that depends on the nature and size of the misalignment and the and of the selected tracks.

# Primary Vertex Validation : $d_{xy}$ and $d_z$ vs $\varphi$



The distance in the transverse ( $d_{xy}$ ) and longitudinal ( $d_z$ ) plane of the track at its closest approach to a refit unbiased primary vertex is studied in bins of track azimuth  $\varphi$  using a sample of 1 million collision events collected by the CMS detector at full magnetic field (3.8T) selected online through minimum bias triggers. The performance of a dedicated alignment achieved with the Millepede-II and HipPy algorithms using cosmic ray and collision data at 3.8T is compared to the one of the alignment used to reprocess the collision data collected by CMS during 2015.

# Primary Vertex Validation : $d_{xy}$ and $d_z$ vs $\eta$



The distance in the transverse ( $d_{xy}$ ) and longitudinal ( $d_z$ ) plane of the track at its closest approach to a refit unbiased primary vertex is studied in bins of track pseudo-rapidity  $\eta$  using a sample of around 1M events collected by the CMS detector at full magnetic field (3.8T) selected online through minimum bias triggers. The performance of a dedicated alignment achieved with the Millepede-II and HipPy algorithms using cosmic ray and collision data at 3.8T is compared to the one of the alignment used to reprocess the collision data collected by CMS during 2015.



## Monitoring of Pixel-Detector High-Level-Structure Movements (PCL Pixel-Alignment)

CMS is employing an automatic procedure to continuously monitor movements of the high-level structures of the pixel tracker ([CMS Collaboration 2014 JINST 9 P06009](#)), which occur for example due to temperature changes or changes of the magnetic field.

For each run with more than 20,000 events, an alignment of the high-level structures is performed online, measuring the movements relative to the geometry used in data processing. When appropriate, the geometry is updated with the results of this online alignment.

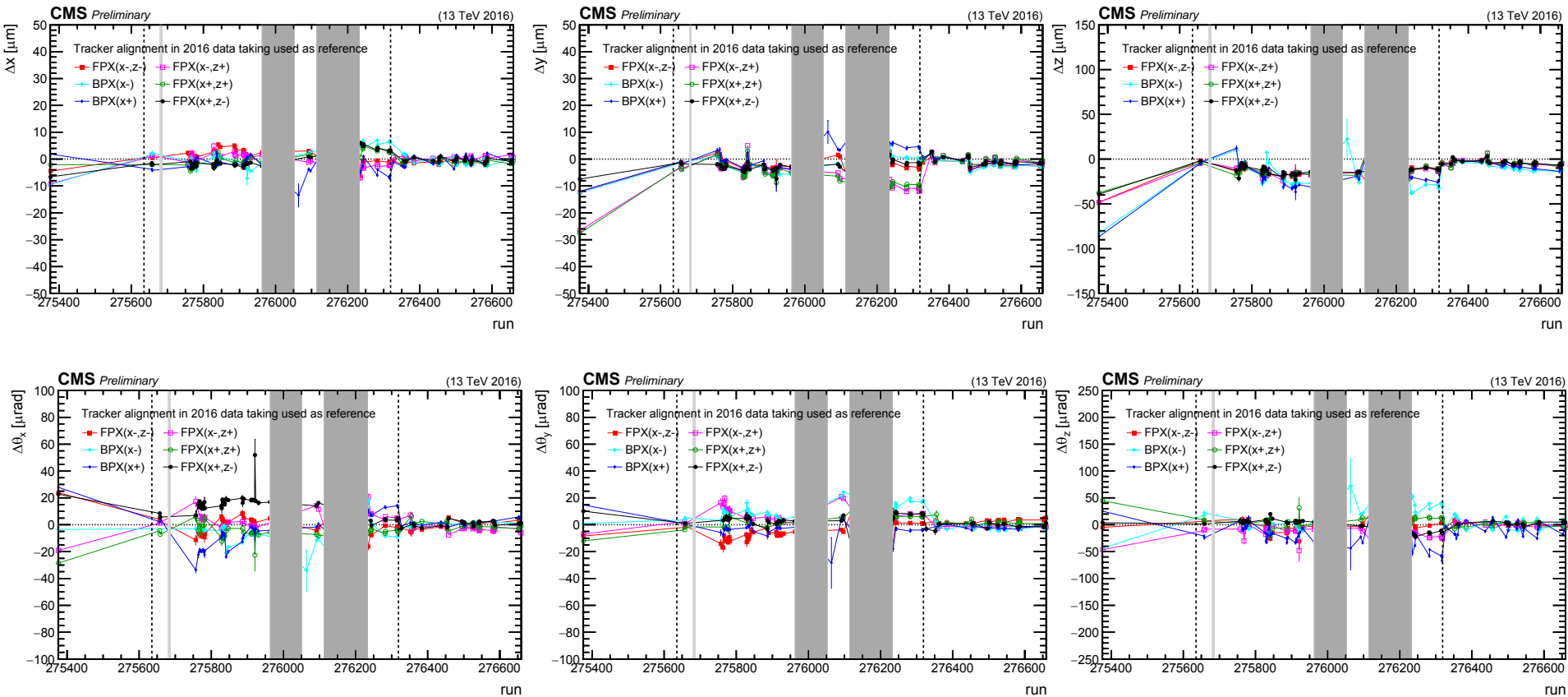
## Evolution of the High-Level-Structure Movements

Observed movements of the high-level structures of the pixel detector monitored as a function of run number.

The run range covers the time from June 21 to July 12 2016, and the recorded data corresponds to an integrated luminosity of 7/fb. Error bars represent the statistical uncertainties of the measurement. Grey bands represent runs during which CMS magnet was not at 3.8T. Vertical dashed lines illustrate updates of the pixel high-level structure reference geometry, after which the mis-alignment is cured.

Typical movements during magnet-off periods are smaller than 50  $\mu\text{m}$  in x and y, and smaller than 150  $\mu\text{m}$  in z. These movements are mostly recovered after a magnet cycle, but this is not expected.

# Time Evolution of the High-Level-Structure Movements

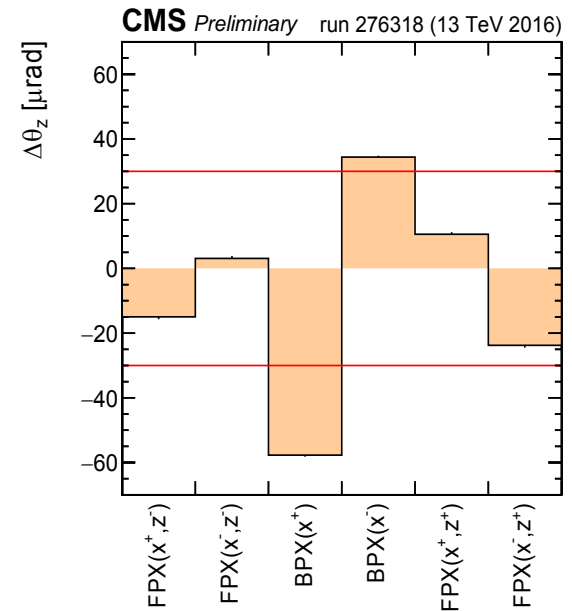
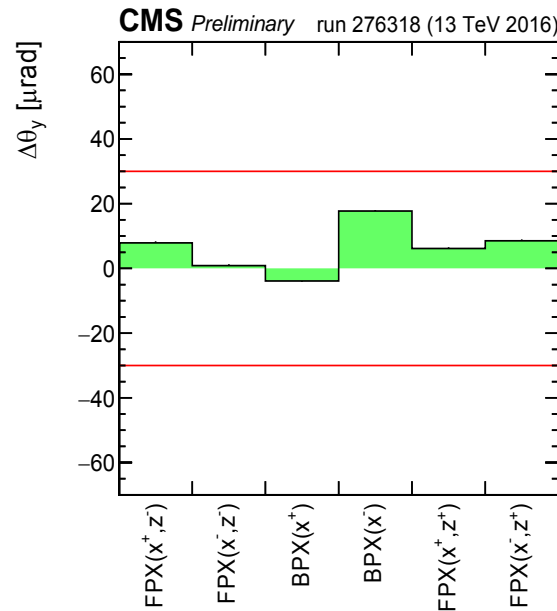
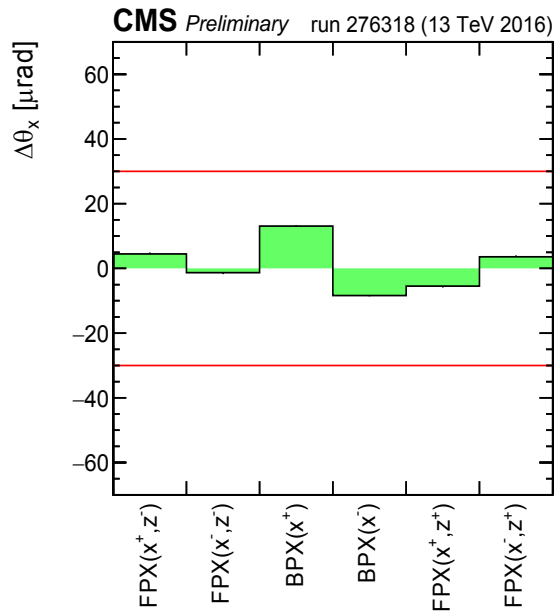
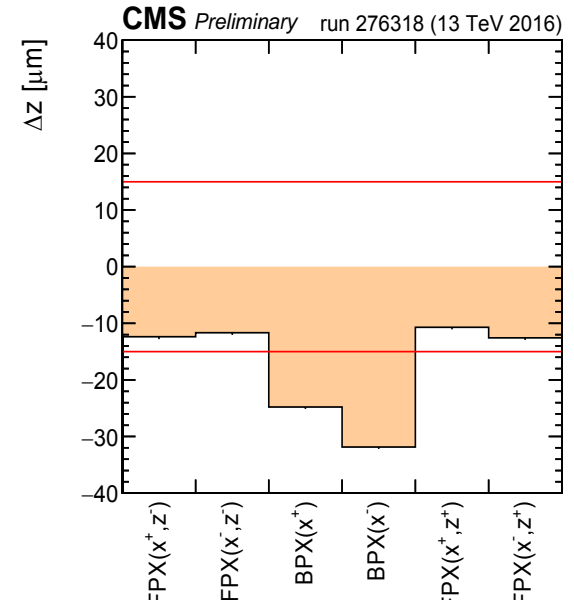
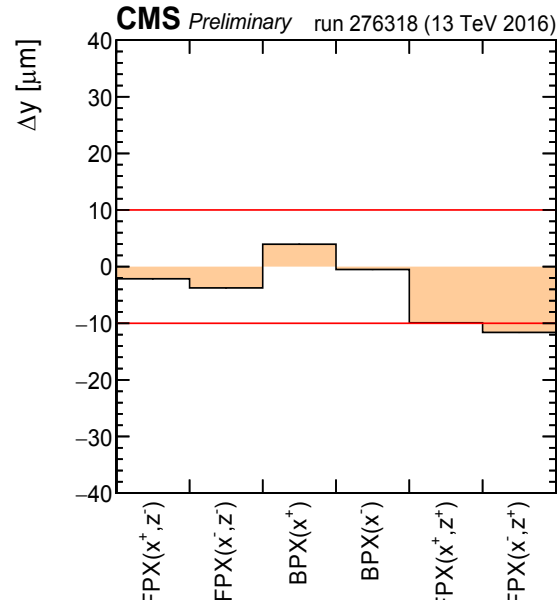
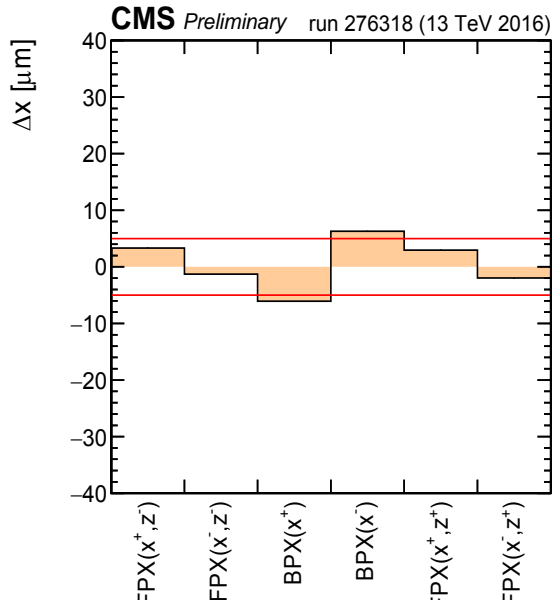


## Per-Run Results

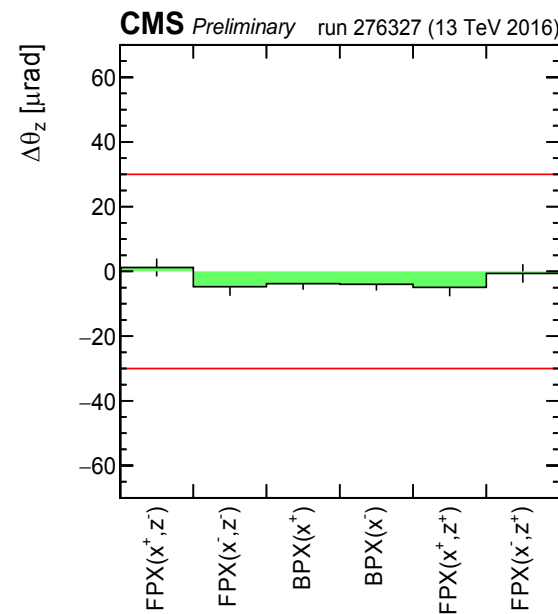
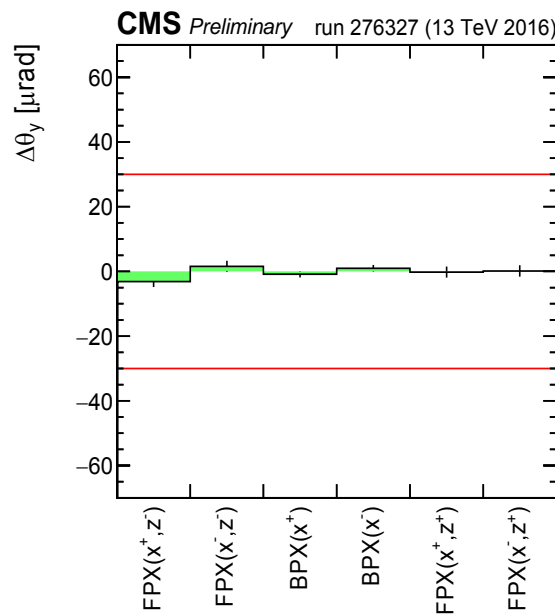
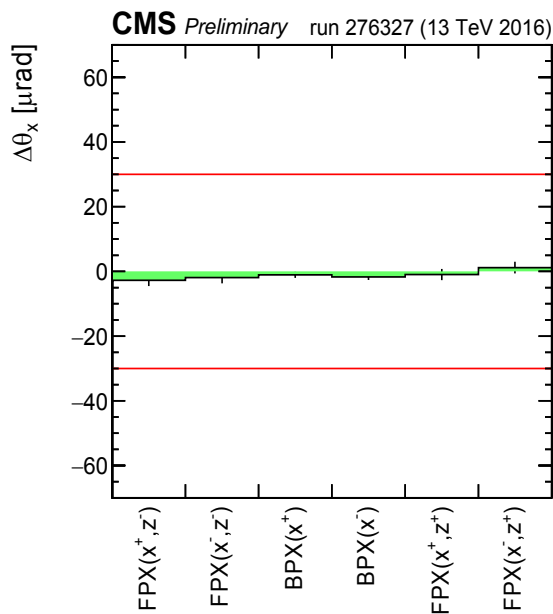
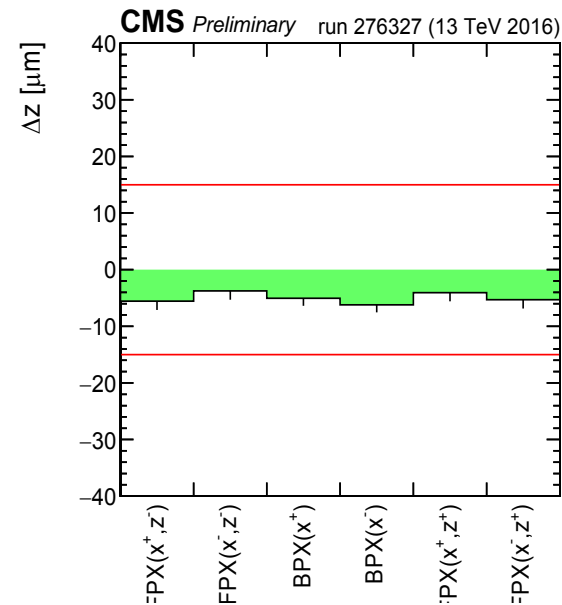
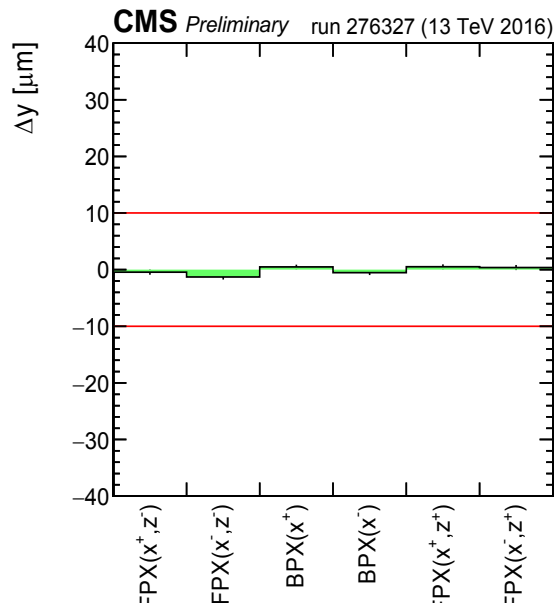
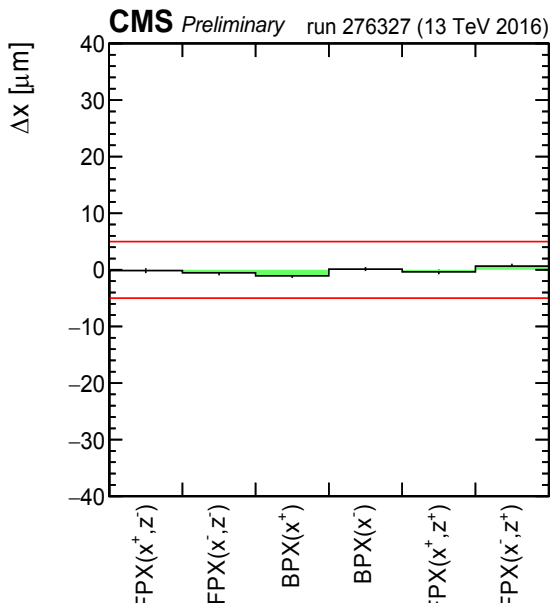
Example of the results of the automatic alignment procedure for two runs taken during July 4 2016. The run 276318 was taken shortly after a magnet ramp, which resulted in movements of the pixel detector structures up to  $30\ \mu\text{m}$  with respect to the geometry used in data processing. The geometry was updated afterwards, leading to a much improved performance during run 276327, where only small residual movements below  $2\ \mu\text{m}$  in  $x$  and  $y$  and below  $10\ \mu\text{m}$  in  $z$  direction are observed.

Such plots are routinely produced per run as part of the data-quality monitoring infrastructure at CMS. The red horizontal lines indicate the limits up to where movements are considered acceptable. If larger movements are observed, an update of the geometry is considered necessary. This is also indicated by the histogram color changing from green to orange if the limit is exceeded. Error bars represent the statistical uncertainties of the measurement.

# First Run after Magnet Ramp



# Next Run: Results after Update



# References

- [1] CMS Collaboration "Alignment of the CMS tracker with LHC and cosmic ray data" 2014 JINST 9 P06009 [doi:10.1088/1748-0221/9/06/P06009](https://doi.org/10.1088/1748-0221/9/06/P06009)
- [2] CMS Collaboration "Alignment of the CMS silicon tracker during commissioning with cosmic rays" 2010 JINST 5 T03009 [doi:10.1088/1748-0221/5/03/T03009](https://doi.org/10.1088/1748-0221/5/03/T03009)